The final publication is available at

https://doi.org/10.1109/ISMICT.2019.8743813

Additional Information

Analysis of the Localization Error for Capsule Endoscopy Applications at UWB Frequencies

Martina Barbi, Sofia Pérez-Simbor, Concepcion Garcia-Pardo and Narcís Cardona
Institute of Telecommunications and Multimedia Applications (ITeAM)
Universitat Politècnica de València
Valencia, Spain
email: {marbar6, sopresim, cgpardo, ncardona} @iteam.upv.es

Abstract— **Localization for Wireless Capsule Endoscopy (WCE) in the Ultra-Wideband frequency band is a very active field of investigation due to its potential advantages in future endoscopy applications. Received Signal Strength (RSS) based localization is commonly preferred due to its simplicity. Previous studies on Ultra-Wideband (UWB) RSS-based localization showed that the localization accuracy depends on the average ranging error related to the selected combination of receivers, which not always is the one experiencing the highest level of received power. In this paper the tendency of the localization error is further investigated through supplementary software simulations and previously conducted laboratory measurements. Two-dimensional (2D) and three-dimensional (3D) positioning are performed and the trend of the localization error compared in both cases. Results shows that the distribution of the selected path loss values, corresponding to the receivers used for localization, around the in-body position to estimate also affects the localization accuracy.**

Keywords— **Wireless capsule endoscopy (WCE), Ultra-Wideband (UWB), in-body localization, heterogeneous phantom-based measurements, CST simulations**

I. INTRODUCTION

Wireless Capsule Endoscopy (WCE) provides a non-invasive and painless way to visualize and diagnose diseases affecting the entire gastrointestinal (GI) tract. Despite the significant advantages, WCE has also limitations. Besides possible complications during the procedure, the images sent to the recorder are not very high quality [1] and moreover, physicians have very little or no information about the exact location of detected disorders. Precise localization of potential abnormalities is crucial for the subsequent treatment through surgery or drug delivery.

Several approaches exist in literature to locate the capsule endoscope: radio frequency (RF) based methods [2], [3], techniques based on magnetic fields [4], [5] and image processing algorithms [6], [7]. One of the most efficient approach is using the RF signal that the capsule also uses to send images, in order to keep the hardware of the WCE simple.

Among the RF-based localization techniques the Received Signal Strength metric is commonly preferred for its simplicity and less sensitivity to bandwidth limitations [8],

[9], [10] with respect to time-based metrics such as time of arrival (ToA) [8], [11] or time difference of arrival (TDoA) [11]. In this case, ranging estimation is performed through a predefined path loss model which describes the attenuation of the RF signal as a function of the distance from the in-body source.

In recent years the Ultra-Wideband (UWB) frequency band [12] has been under investigation to improve the quality of the images sent by the capsule which is currently very poor [1] using the standardized Medical Implant Communication System (MICS) frequency band.

Studies involving RF-based localization at UWB frequencies are quite limited in literature. Analysis conducted through electromagnetic simulators as well as through experimental measurements using a homogeneous phantom are presented in [9], [13], [14], [15]. However, none of them investigates the impact of the on-body receivers configuration on the localization performance. In one of our previous study on RSS-based WCE two-dimensional (2D) localization at UWB frequencies, using laboratory measurements [16], results showed that the lowest localization error was achieved using the combination of receivers experiencing the highest level of received power, which is in line with the current way localization is performed within the software platform, provided to the hospitals [17], [18]. Nevertheless, in our recent work on three-dimensional (3D) WCE localization through simulations and *in vivo* measurements [19], results pointed out that this condition is not always satisfied. Particularly, it was found that the localization accuracy improves if the ranging error, on average, decreases, regardless of whether the selected receivers are experiencing the highest power or not. In order to better investigate this tendency, more simulations were carried out and are presented in this paper. RSS-based localization performances are then compared for the three-dimensional (3D) and two-dimensional (2D) case to assess the behavior of the localization error.

The remainder of the paper is organized as follows: Section II summarizes the laboratory measurements testbed as well as the simulation-based setup. Section III briefly presents the RSS-based localization algorithms used for two-dimensional and three-dimensional localization. Performance metrics and results are presented in Section IV. Finally, conclusions and future plans are discussed in Section V.

II. MEASUREMENTS SETUP

A. Laboratory measurements

Experimental measurements, in laboratory, using a heterogeneous phantom model were conducted in the 3.1 –

8.5 GHz UWB frequency band. The customized setup used for the measurements is depicted in Fig. 1.
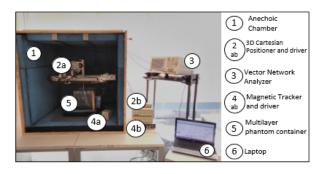

Fig. 1. Laboratory Measurement Setup

In order to emulate the WCE scenario a newly designed multilayer container (Fig. 1, element 5) was filled up with muscle and fat phantom. Muscle-like tissue was used instead of colon or small bowel, due to their similar permittivity, and also because the muscle phantom created at UPV [20] is the most accurate so far among those available in literature.

The S_{21} parameter was measured, considering 3201 resolution points in frequency, by means of a Vector Network Analyzer (Fig. 1, element 3) for different positions of the in-body and on-body antenna. The in-body antenna was moved inside the muscle layer through a 3D Cartesian positioner (Fig. 1, element 2a) in steps of 1 cm along x, y, z axis with grid size of (Nx=12, Ny=11, Nz=2), as shown in Fig. 2. The on-body antenna was placed in five different positions, with a separation of 2 cm, on the outer edge of the fat layer (Fig. 2).
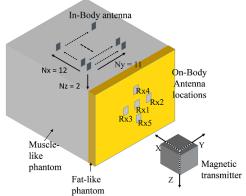

Fig. 2. Measured in-body and on-body positions

The in-body and on-body antenna used for these experimental measurements are UWB omnidirectional patch antennas, designed to operate inside and on the surface of the human body respectively [21], [22].

A magnetic tracker (Fig. 1, element 4ab) was used to precisely evaluate the distance between in-body and on-body antenna as well as their respective (x, y, z) coordinates with respect to the magnetic transmitter reference system (Fig. 2).

Further details regarding the experimental measurements setup can be found in [23].

B. CST-based simulations

Software simulations in the 3.1 – 5.1 GHz UWB frequency band were carried out using CST MICROWAVE STUDIO® (CST MWS). The S_{21} parameter was evaluated by the simulator through the Finite Difference Time Domain (FDTD) method. With the aim of comparing the simulation results to those obtained through laboratory measurements, the abdominal part of a human female CAD model (Nelly) was used in order to mimic the same human tissues (i.e. muscle and fat). No internal organs as well as no blood flow were taken into account to reduce the simulations computational time. The considered model along with the measurements setup is shown in Fig. 3.

Same in-body and on-body antenna used for laboratory measurements and described in Section II.A were used in the simulations.
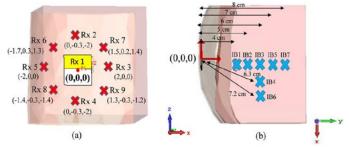

Fig. 3. On-body (a) and in-body (b) antenna locations (top view)

The S_{21} parameter was calculated by moving the in-body antenna in seven different positions inside the muscle layer (Fig. 3(b)) for nine different on-body locations (Fig. 3(a)) on the abdominal region of the CAD model.

In this case, the center (P1) of Rx1 (Fig. 3(a)) is taken as the origin of the reference system used to evaluate the real and the estimated coordinates of the in-body antenna.

III. RSS-BASED LOCALIZATION

For both, laboratory measurements and CST-based simulations, data corresponding to antenna distances up to 8 cm and to frequencies from 3.1 to 5.1 GHz were taken into account to ensure that all considered measurements are well above the noise level [23]. For each in-body to on-body antenna location the path loss is evaluated as:

$$PL_{meas}(dB) = -10\log_{10}\left(mean\left(\left|H(f)\right|^2\right)\right) \qquad (1)$$

where *H(f)* is the frequency-domain transfer function in N resolution points computed as $H(f) = |S_{21}|e^{-j\phi_{S_{21}}}$, being $|S_{21}|$ and $\phi_{S_{21}}$ module and phase in radians of the S_{21}, respectively. Only S_{21} values above the noise level (-90 dB) were considered.

The log-distance approximation model derived from the fitting of the path loss values calculated through (1) can be expressed as:

$$PL(dB) = PL_{0,d_{ref}}(dB) + 10n\log_{10}\left(\frac{d}{d_{ref}}\right) \qquad (2)$$

where *d* is the distance between antenna centers, d_{ref} is the reference distance at 1 cm, $PL_{0,d_{ref}}$ is the path loss at d_{ref} and *n* is the path loss exponent.

The distance between antennas, using the model given in (2), can be estimated as:

$$d_{est} = 10^{\frac{PL_{meas} - PL_{0,dref}}{10n}} \cdot d_{ref} \qquad (3)$$

where PL_{meas} is the path loss evaluated using (1).

For the phantom-based measurements, only two coordinates of the in-body antenna (y and z) could be estimated as all measured on-body positions (also referred as receivers) share the same x-coordinate (Fig. 2). In this case, the adaptive linearized method in [24] has been adapted [16] for two dimensional positioning. In this approach, a minimum of three receivers (one of them taken as reference) is needed to find the unique solution (y and z coordinate of the in-body antenna) of the linearized system of two equations in two unknowns.

For the CST-based simulations, three-dimensional positioning has been performed by selecting combinations of more than four receivers. In this case, the coordinates of the in-body antenna are estimated using the Non Linear Least Square (NLLS) approach [25], where the sum of the square errors is minimized through the Levenberg-Marquardt algorithm [26]. Further details regarding the selection criteria of the receivers are given in Section IV.

IV. RESULTS

Localization results were evaluated according to the relative localization error metric. For 3D positioning the Localization Error (LE) and its corresponding relative error can be defined as:

$$LE = \sqrt{\left(x_{IB} - x_{IB\_est}\right)^2 + \left(y_{IB} - y_{IB\_est}\right)^2 + \left(z_{IB} - z_{IB\_est}\right)^2} \qquad (4)$$

$$RelLE = \frac{LE}{\sqrt{x_{IB}^2 + y_{IB}^2 + z_{IB}^2}} \qquad (5)$$

where (x_{IB}, y_{IB}, z_{IB}) and $(x_{IB\_est}, y_{IB\_est}, z_{IB\_est})$ are the real and estimated coordinates of the in-body antenna, respectively.

For two-dimensional positioning (4) and (5) are calculated omitting the x-coordinate because only y and z could be estimated due to the receivers configuration (Fig. 2).

Furthermore, for the analysis of the localization error tendency, the average ranging error for each considered in-body position can be evaluated as:

$$Avg_{Ranging\_Error} = \frac{\sum_{i=1}^{N_{Rxs}} |d_i - d_{i,est}|}{N_{Rxs}} \qquad (6)$$

where N_{Rxs} is the number of receivers used for positioning, d_i is the real distance between the in-body antenna and the ith receiver and $d_{i,est}$ is the estimated distance between the in-body antenna and the ith receiver, obtained through (3).

A. 3D positioning results

From CST-based simulations, path loss parameters $PL_{0,dref}$=-10.34 dB and n=9.79 of the log-distance fitting model were obtained, considering a reference distance of d_0=1 cm.

Localization is performed, by selecting the receivers experiencing the highest level of received power, firstly starting with four and then increasing the number up to nine.

Fig. 4 shows the relative localization error, evaluated as in (5), obtained for the seven in-body positions depicted in Fig. 3, using an increasing number of receivers. The actual in-body antenna location reported on the x-axis, in Fig. 4 represents the distance between the origin of the reference system (center of Rx1 in Fig. 3) and the considered in-body antenna positions.
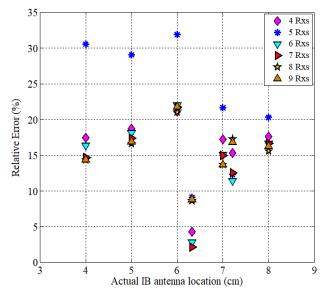

Fig. 4. 3D relative localization error vs actual in-body antenna location

It can be observed, in Fig. 4, that increasing the number of receivers experiencing the highest level of received power, not always leads to lower localization errors, as it was formerly concluded in [19].

For all seven in-body positions an increment in the average ranging error, calculated as in (6), mostly result in a higher localization error and vice versa [19]. However, this is true not for all cases represented in Fig. 4, as shown in Table I and Table II, which report for each in-body position under study the 3D localization error and the average ranging error obtained with different combinations of receivers. In fact, for in-body position at 6 cm (IB3), for example, passing from 4 to 5 receivers the average ranging error slightly decreases and the localization error increases. The same happens for in-body position at 8 cm (IB7) passing from eight to nine receivers.

The opposite behavior is observed for in-body position at 7.2 cm (IB6) where an increment in the average ranging error results in a lower localization error, passing from 4 to 5 receivers.

TABLE I
3D LOCALIZATION & AVG RANGING ERRORS FOR IB1 TO IB4

Nr of Rxs	IB1 (4 cm)		IB2 (5 cm)		IB3 (6 cm)		IB4 (6.3 cm)	
	LE (%)	Avg RE (cm)	LE (%)	Avg RE (cm)	LE (%)	Avg RE (cm)	LE (%)	Avg RE (cm)
4	17.46	0.06	18.72	0.10	21.12	0.12	4.28	0.08
5	30.56	0.07	29.05	0.11	31.91	0.11	9.12	0.10
6	16.36	0.06	18.13	0.11	22.01	0.10	2.82	0.10
7	14.69	0.06	17.39	0.10	21.74	0.09	2.14	0.09
8	14.36	0.06	16.63	0.10	21.05	0.09	8.64	0.10
9	14.40	0.06	16.91	0.10	21.78	0.11	8.82	0.16

Nr of Rxs	IB5 (7 cm)		IB6 (7.2 cm)		IB7 (8 cm)	
	LE (%)	Avg RE (cm)	LE (%)	Avg RE (cm)	LE (%)	Avg RE (cm)
4	17.23	0.05	15.32	0.53	17.62	0.45
5	21.67	0.07	12.30	0.55	20.32	0.47
6	15.08	0.08	11.42	0.49	16.62	0.46
7	14.97	0.09	12.56	0.43	16.66	0.47
8	13.72	0.11	17.29	0.53	15.62	0.47
9	13.66	0.10	16.80	0.52	16.27	0.43

The behavior of the localization error, taking as example in-body antenna positon IB3 and IB6 can be explained by looking, in Fig. 5, at the dispersion of the path loss values, corresponding to the selected four/five receivers used for positioning, with respect to the log-distance fitting model. For in-body position IB3 (Fig. 5(a)), passing from four (magenta diamond) to five receivers (blue dots) the average ranging error decreases because the selected path loss values are all in close proximity. Since they are not uniformly distributed around the position to estimate (6 cm) adding one more receiver does not increase the diversity of the estimated ranging distances (all values are very close to each other) used for localization.
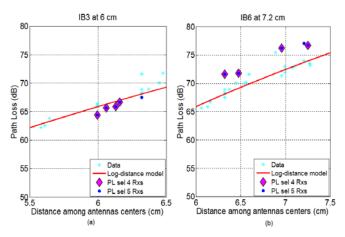

Fig. 5. Simulated path loss values and fitting model along with path loss values of selected receivers for in-body position at 6 cm (a) and at 7 cm (b)

For in-body position at 7.2 cm, (Fig. 5(b)), adding one more receiver increases the diversity of the estimated ranging distances used for localization as the selected path loss values are more evenly distributed around the position to estimate (7.2 cm). One reason for this behavior could be the minimization error algorithm, used to evaluate the in-body antenna coordinates. In order to confirm this supposition, 2D localization was performed for similar antenna distances and positons. More details regarding the 2D results are given in the following section.

B. 2D positioning results

From 2D laboratory measurements, path loss parameters $PL_{0,dref}$ =-24.43 dB and n=9.69 of the log-distance fitting model were obtained considering a reference distance of d_0=1 cm and antennas distances up to 8 cm.

As mentioned in the previous section, in order to verify the behavior observed for 3D software simulations, 2D positioning was performed. In this case, the in-body antenna coordinates are evaluated by simply solving a linear system in two unknown, using three receivers [15] so the localization error does not depend on the optimization algorithm. With the aim of comparing the tendency of the localization error in both cases (2D and 3D), the in-body antenna locations corresponding to the grid points which are more aligned with respect to the central on-body receiver (Rx1 in Fig. 2) were considered. Fig. 6 depicts the relative localization error, calculated as in (5), of these selected in-body positions for different combinations of three receivers.
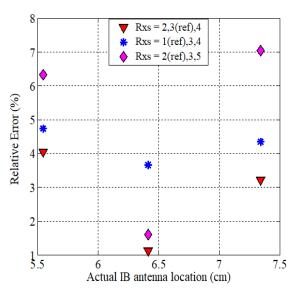

Fig. 6. 2D relative localization error vs actual in-body antenna location for different combinations of three receivers

The in-body antenna location reported on the x-axis, in Fig. 6 represents the distance between the central receiver, Rx1, in Fig. 2 and the considered in-body antenna positions. It can be observed, in Fig. 6, that for all the considered in-body positions the lowest error is achieved using the combination of receivers 2, 4 and 3, taken as reference. This combination of receivers is experiencing on average, per in-body position, the highest level of received power. Nevertheless, the corresponding average ranging error per in-body position, evaluated as in (6), is not the lowest as shown in Table III, which reports for each in-body position under study the 2D localization error along with the average ranging error, for the three considered combinations of receivers.

Rxs	IB1 (5.5 cm)		IB2 (6.4 cm)		IB3 (7.3 cm)	
	LE (%)	Avg RE (cm)	LE (%)	Avg RE (cm)	LE (%)	Avg RE (cm)
2,3(ref),4	4.05	0.31	1.12	0.24	3.21	0.26
1(ref),3,4	4.74	0.21	3.66	0.12	4.35	0.16
2(ref),3,5	6.33	0.27	1.60	0.28	7.04	0.34

The lowest average ranging error is indeed achieved by the combination of receivers 3, 4 and 1 taken as reference.
This tendency of the localization error is the same observed for the 3D case, therefore the minimization algorithm is not the main cause of this behavior.
As for the 3D case, the dispersion of the path loss values, corresponding to the selected combinations of receivers, with respect to the fitting model curve has been analyzed and is depicted in Fig. 7. The selected path loss values, used for ranging estimation, are grouped per in-body position and are represented for receivers 2, 3 (reference), 4 in Fig. 7(a), for receivers 1 (reference), 3, 4 in Fig. 7(b) and for receivers

2 (reference), 3, 5 in Fig. 7(c), respectively. The yellow stars on the x-axis illustrates the actual positions of the in-body antenna to estimate.
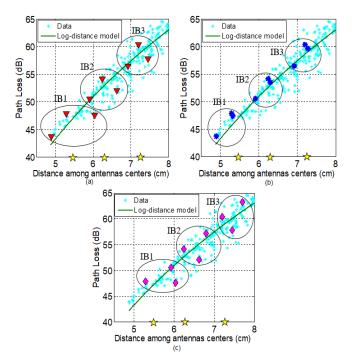

Fig. 7. Measured path loss values and fitting model along with path loss values related to receivers 2,4,3(ref) (a) to receivers 1(ref),3,4 (b) to receivers 2(ref),3,5 (c) for in-body position at 5.52 cm, 6.39 cm and at 7.32 cm

Looking at Fig. 7, same behavior as for the 3D case is observed. Using the combination of receivers 2, 3 (reference) and 4 (Fig. 7(a)) the selected path loss values used for ranging estimation are more uniformly distributed around the position to estimate, compared to the other combinations of receivers (Fig. 7(b) and Fig. 7(c)). This means more diversity among the estimated ranging distances values, used for localization. Using the combination of receivers 1 (reference), 3 and 4, (Fig. 7(b)), the average ranging error is minimized but two of the selected path loss values are very close to each other, leading to similar estimates of the ranging distance.
These results point out that the average ranging error metric alone is not enough to ensure that the localization error should increase or decrease. As a matter of fact, the distribution of the selected path loss values around the in-body position to estimate also affects the localization accuracy, as likewise observed for the 3D case, in the previous section.

V. CONCLUSIONS

Previous results on RSS-based positioning for UWB capsule endoscopy applications showed that the localization accuracy depends on the average ranging error, corresponding to the selected combination of receivers used for localization. In this paper the tendency of the localization error has been further investigated through supplementary software simulations and previously conducted laboratory measurements. Results obtained for two-dimensional and three-dimensional positioning, show that, not only the average ranging error, but also the distribution of the selected path loss values, corresponding to the receivers used for localization, around the position to estimate affects the

localization accuracy. Particularly, from the obtained results, it seems that for more uniformly distributed values, the positioning accuracy increases.

As part of future plans, more extensive measurement campaigns, in laboratory as well as *in vivo* and through simulations, will be conducted to achieve a more general conclusion regarding the position and the minimum number of selected receivers leading to an acceptable localization error for capsule endoscopy applications.

REFERENCES

[1] G. Ciuti, A. Menciassi, and P. Dario, "Capsule Endoscopy : From Current Achievments to Open Challenges," *IEEE Trans. Biomed. Eng.*, vol. 4, pp. 59–72, 2011.

[2] K. Pahlavan *et al.*, "RF localization for wireless video capsule endoscopy," *Int. J. Wirel. Inf. Networks*, vol. 19, no. 4, pp. 326–340, 2012.

[3] M. Pourhomayoun, M. Fowler, and Z. Jin, "A novel method for medical implant in-body localization," in *Proceedings of the Annual International Conference of the IEEE Engineering in Medicine and Biology Society, EMBS*, 2012, pp. 5757–5760.

[4] C. Hu, M. Q. Meng, and M. Mandal, "Efficient Magnetic Localization and Orientation Technique for Capsule Endoscopy," in *IEEE/RSJ International Conference on Intelligent Robots and Systems*, 2005, pp. 3365–3370.

[5] R. Kuth, J. Reinschke, and R. Rockelein, "Method for determining the position and orientation of an endoscopy capsule guided through an examination object by using a navigating magnetic field generated by means of a navigation device," US20070038063, 2007.

[6] G. Bao, L. Mi, and K. Pahlavan, "A Video Aided RF Localization Technique for the Wireless Capsule Endoscope (WCE) inside Small Intestine," in *Proceedings of the 8th International Conference on Body Area Networks*, 2013, no. February 2016, pp. 55–61.

[7] G. Bao and K. Pahlavai, "Motion estimation of the endoscopy capsule using region-based Kernel SVM classifier," in *IEEE International Conference on Electro Information Technology*, 2013.

[8] U. I. Khan, K. Pahlavan, and S. Makarov, "Comparison of TOA and RSS based techniques for RF localization inside human tissue," in *Proceedings of the Annual International Conference of the IEEE Engineering in Medicine and Biology Society, EMBS*, 2011, pp. 5602–5607.

[9] A. S. Bjørnevik, "Localization and Tracking of Intestinal Paths for Wireless Capsule Endoscopy," M. S. Thesis, DET, Norwegian University of Science and Technology, 2015.

[10] H. Farhadi, J. Atai, M. Skoglund, E. S. Nadimi, K. Pahlavan, and V. Tarokh, "An adaptive localization technique for wireless capsule endoscopy," *Int. Symp. Med. Inf. Commun. Technol. ISMICT*, vol. 2016–June, pp. 1–5, 2016.

[11] A. R. Nafchi, S. T. Goh, and S. A. R. Zekavat, "Circular arrays and inertial measurement unit for DOA/TOA/TDOA-based endoscopy capsule localization: Performance and complexity investigation," *IEEE Sens. J.*, vol. 14, no. 11, pp. 3791–3799, 2014.

[12] Q. W. Jianqing Wang, *Body Area Communications: Channel Modeling, Communication Systems, and EMC*. 2013.

[13] B. Moussakhani, J. T. Flåm, S. Støa, I. Balasingham, and T. Ramstad, "On localisation accuracy inside the human abdomen region," *IET Wirel. Sens. Syst.*, vol. 2, no. 1, pp. 9–15, Mar. 2012.

[14] M. Kanaan and M. Suveren, "In-body ranging with ultra-wideband signals: Techniques and modeling of the ranging error," *Wirel. Commun. Mob. Comput.*, vol. 2017, 2017.

[15] Y. Ye, "Bounds on Rf Cooperative Localization for Video Capsule Endoscopy," Ph.D. dissertation, ECE, WPI, Worcester, MA, USA, 2013.

[16] M.Barbi, S. Perez-Simbor, C. Garcia-Pardo, C. Andreu, N. Cardona, "Localization for Capsule Endoscopy at UWB Frequencies using an Experimental Multilayer Phantom," in IEEE Wireless Communications and Networking Conference, WCNC, 2018, Barcelona, Spain.

[17] T. D. Than, G. Alici, H. Zhou and W. Li, "A Review of Localization Systems for Robotic Endoscopic Capsules," *IEEE Trans. Biomed. Eng.*, vol. 59, no. 9, 2012.

[18] M. R. Basar, F. Malek, K. M. Juni, M. S. Idris, and M. I. M. Saleh, "Ingestible wireless capsule technology: A review of development and future indication," *Int. J. Antennas Propag.*, vol. 2012, 2012.

[19] M. Barbi, C. Garcia-Pardo, N. Cardona, A. Nevarez, V. Pons and M.

Frasson, "Impact of Receivers Location on the Accuracy of Capsule Endoscope Localization," in *IEEE 29th Annual International Symposium on Personal, Indoor and Mobile Radio Communications PIMRC,* 2018, Bologna, Italy, pp. 340-344.

[20] N. Cardona, S. Castello-Palacios, A. Fornes-Leal, C. Garcia-Pardo, and A. Valles-Lluch, "Synthetic Model of Biological Tissues for Evaluating the Wireless Transmission of Electromagnetic Waves," Patent WO/2017/109252, 30-Jun-2017.

[21] C. Andreu, C. Garcia-Pardo, A. Fornes-Leal, M. Cabedo-Fabrés, and N. Cardona, "UWB In-Body Channel Performance by Using a Direct Antenna Designing Procedure," in *11th European Conference on Antennas and Propagation (EUCAP)*, 2017, p. 5.

[22] C. Tarín, P. Martí, L. Traver, N. Cardona, J. A. Díaz, and E. Antonino, "UWB channel measurements for hand-portable devices: A comparative study," in *IEEE International Symposium on Personal, Indoor and Mobile Radio Communications, PIMRC*, 2007.

[23] S. Perez-Simbor, M. Barbi, C. Garcia-Pardo, S. Castello-Palacios, N. Cardona, "Initial UWB in-body channel characterization using a novel multilayer phantom measurement setup," in IEEE Wireless Communications and Networking Conference, WCNC, 2018, Barcelona, Spain.

[24] K. Arshak and F. Adepoju, "Adaptive linearized methods for tracking a moving telemetry capsule," *IEEE Int. Symp. Ind. Electron.*, pp. 2703–2708, 2007.

[25] W. Murphy and W. Hereman, "Determination of a position in three dimensions using trilateration and approximate distances," *Department of Mathematical and Computer Sciences, Colorado School of Mines, Golden, Colorado, MCS-95*, vol. 7. p. 19, 1995.

[26] Charles L. Lawson and Richard J. Hanson, *Solving Least Squares Problems*. 1995.